

Purdue University

Purdue e-Pubs

International Refrigeration and Air Conditioning
Conference

School of Mechanical Engineering

2022

Effect of Lubricating Oil on the Refrigerant Heat Transfer Performance during Spray Evaporation on Tube Bundles

Jerin Robins Ebanesar

Lorenzo Cremaschi

Follow this and additional works at: <https://docs.lib.purdue.edu/iracc>

Ebanesar, Jerin Robins and Cremaschi, Lorenzo, "Effect of Lubricating Oil on the Refrigerant Heat Transfer Performance during Spray Evaporation on Tube Bundles" (2022). *International Refrigeration and Air Conditioning Conference*. Paper 2328.
<https://docs.lib.purdue.edu/iracc/2328>

This document has been made available through Purdue e-Pubs, a service of the Purdue University Libraries. Please contact epubs@purdue.edu for additional information. Complete proceedings may be acquired in print and on CD-ROM directly from the Ray W. Herrick Laboratories at <https://engineering.purdue.edu/Herrick/Events/orderlit.html>

Effect of Lubricating Oil on the Refrigerant Heat Transfer Performance during Spray Evaporation on Tube Bundles

Jerin Robins EBANESAR^{1*}, Lorenzo CREMASCHI²

Auburn University, Mechanical Engineering,
Auburn, Alabama, USA

¹(+13345246481, jre0028@auburn.edu)

²(+13348443302, lzc0047@auburn.edu)

* Corresponding Author

ABSTRACT

This paper describes the effect of lubricating oil on the heat transfer performance of spray evaporators for air conditioning and refrigeration systems. The literature on low-GWP refrigerants and oil mixtures is limited for these types of heat exchangers. The present paper provides new heat transfer coefficient data for tube bundles that adopted enhanced outer tube surfaces. The experiments were carried out for refrigerant and lubricant mixtures of R134a (HFC) and R1234ze(E) (HFO) with synthetic polyester (POE) and polyether (PE) lubricants. The effects of heat flux, oil viscosity, oil circulation ratio (OCR), and saturation temperature were presented. The saturation temperature ranged from -9°C to 10°C (16°F to 50°F), and the heat flux varied between 3 kW/m² and 20 kW/m². The results indicated a slight decrease of the tube bundle heat transfer coefficient for OCRs of less than 1%. In some testing conditions, the small amount of lubricant in the spray enhanced the tube bundle heat transfer coefficient by as much as 10 percent. However, if the OCRs were higher than 1%, marked penalizations of the heat transfer coefficient were measured, particularly at low saturation evaporation temperature.

1. INTRODUCTION

Greenhouse gas emissions from refrigeration systems can be classified into direct and indirect. Indirect emission comes from the powering of the system. Direct emissions are due to refrigerants leaked into the environment during the production process from refrigerant banks and during the end-of-life disposal of appliances. Direct emissions can be controlled by producing a small amount of refrigerant and using alternative low global warming potential (GWP) refrigerants that still provide similar system efficiency as conventional type refrigerants. Hydrofluoroolefins (HFOs) are Low GWP refrigerants that will break down in a matter of days during their stay in the environment. To reduce refrigerant usage and promote efficiency, flooded-type evaporators can be replaced with spray-type evaporators. Thus, using low-GWP refrigerants with spray evaporators in refrigeration systems mitigates the adverse effect of current cooling fluids on global warming.

Spray evaporators are widely used in desalination, refrigeration, petroleum refining, chemical industries, etc. Several experimental investigations on falling film evaporation on horizontal single tube and tube bundles had been conducted in the past. A comprehensive review by Ribatski and Jacobi (2005) touched on most of the design and thermal aspects of falling film evaporation. Recent experimental studies investigated the falling film heat transfer performance of different enhanced tubes using refrigerants as working fluid. Ji *et al.* (2019) reported that at lower heat fluxes, less than 30 kW/m², falling film heat transfer coefficient is higher than that of pool boiling HTC, however, at higher heat flux opposite trend is observed.

R1234ze(E) is an alternative refrigerant proposed to replace R134a at medium and high-pressure applications. Several recent studies have experimentally investigated the pool boiling heat transfer characteristics of R1234ze(E). Rooyen and Thome (2013) studied the pool boiling heat transfer performance of two enhanced surfaces using R134a, R236fa, and R1234ze(E). Nagata *et al.* (2016) experimentally investigated the pool boiling heat transfer characteristics of R1234ze(E), R1234ze(Z), and R1233zd(E) on plain horizontal tubes. It is reported that the heat transfer coefficient of R1234ze(E) is slightly lower than that of R134a. Byun *et al.* (2017) conducted an experimental study to evaluate the

pool boiling heat transfer characteristics of R1234ze(E) and R1233zd(E) on enhanced tubes as well as on plain tubes. Reported a lower heat transfer coefficient for both refrigerants compared to R134a. Another experimental study conducted by Chen *et al.* (2021) investigated the pool boiling HTC of R1234ze(E) and R1233zd(E) on two typical reentrant cavity tubes. It is reported that R1234ze(E) and R134a exhibited equivalent pool boiling HTC.

In contrast to pool boiling experiments, there have been few studies on the falling film evaporation of Low-GWP refrigerants. Jige *et al.* (2019) conducted an experimental study of falling film evaporation of R1234ze(E) and R245fa on horizontal smooth tubes. It is reported that the heat transfer coefficient of R1234ze(E) is higher than that of R245fa at higher heat flux, however, there is no significant difference in heat transfer coefficient at lower heat flux. Sun *et al.* (2021) experimentally investigated the falling film evaporation of R1234ze(E) on two kinds of enhanced tubes and reported a heat transfer enhancement factor of about 2.5 compared to smooth tubes. Ubara *et al.* (2021) experimentally investigated the falling film heat transfer characteristics of R1233zd(E) and R134a on a thermal spray coated single horizontal tube. Reported a lower heat transfer coefficient for R1233zd(E) compared to R134a and a heat transfer enhancement factor of 2.1 to 4.8 using thermal spray coated tubes. Hassani and Kothukamal (2020) numerically investigated the heat transfer characteristics of R1233zd(E) and R245fa. A 2D laminar unsteady model with VOF scheme for interface tracking is developed. Successfully implemented and validated the mass transfer model up to a wall superheat of 7 K.

Oil is often used in vapor compression systems for lubricating the moving parts in the compressor. If not removed completely, the oil will flow through the heat exchangers and other components of the system. In heat exchangers, this will affect the flow pattern and both the heat transfer and pressure drop depending on the concentration. In general, oil circulation in the system can vary from 0.1% to 8% (Bandarra *et al.*, 2009, Bolaji and Huan, 2013). Gibb *et al.* (2003) reported that proper lubrication can bring down the energy consumption of the compressor by 15%. Chien *et al.* (2019) conducted experimental studies to investigate the effects of lubricating oil on falling film evaporation of R245fa/oil mixtures. An experimental study by Minxia *et al.* (2021) investigated the falling film heat transfer coefficient of R134a/oil mixture on three different tubes. There is no published literature on falling film evaporation with low-GWP refrigerants/oil mixtures. Considering the recent rise in popularity of low-GWP refrigerants and the inescapable influence of lubricating oil, the present study focuses on the effect of lubricating oil on the low-GWP refrigerant heat transfer performance during spray evaporation. Spray evaporation on tube bundle experiments was carried out for refrigerant and lubricant mixtures of R134a (HFC) and R1234ze (HFO) with synthetic polyester (POE) and polyether (PE) lubricants.

2. EXPERIMENTAL STUDY

Test conditions are listed in Table 1. The working fluid is either oil-free R134a and R1234ze or the mixtures with POE and PE lubricants. OCR varied from 1% to 3%. The properties of the lubricants are listed in Table 2.

Table 1: Test parameters.

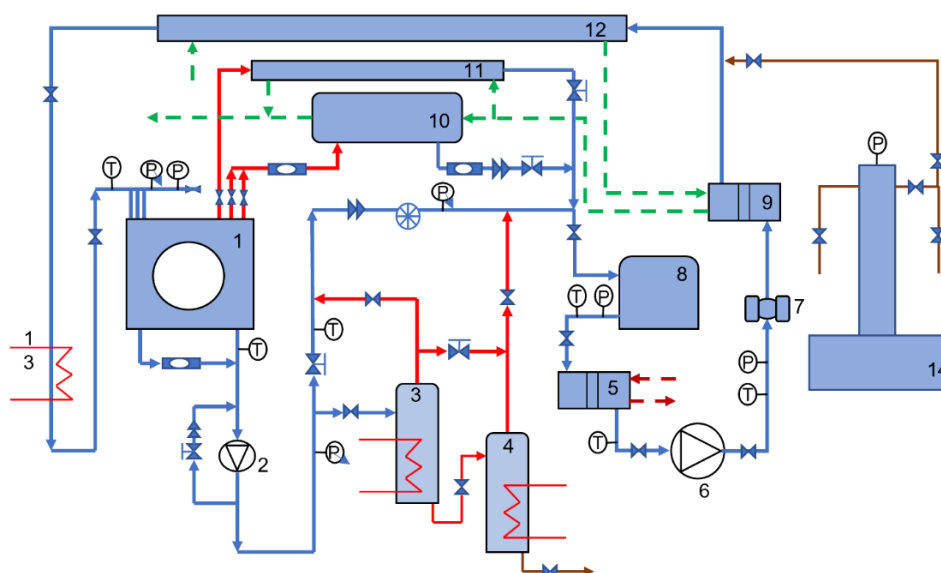
OCR	1 – 3%
Saturation temperature	16, 36, 50°F (-9, 2, 10°C)
Mass flow rate	300 – 750 lbm/hr (0.037 - 0.094 kg/s)
Heat flux	3 – 17 kW/m ²
Subcooling	< 1.1°C (2°F)

Table 2: Properties of the lubricants.

Lubricant Name	Type	Density	Viscosity
Zerol Ester 68	POE (Polyester)	0.964 g/cm ³ at 15°C	68 mm ² /s at 40°C
Zerol Ester 220	POE (Polyester)	0.968 g/cm ³ at 15°C	220 mm ² /s at 40°C 19 mm ² /s at 100°C
Zerol PE 100-x	PE (Polyether)	1.01 g/cm ³ at 20°C	104.1 mm ² /s at 40°C 18.7 mm ² /s at 20°C

2.1 Test Facility

Figure 1 shows the experimental apparatus which consists of refrigerant, EGW, and Syltherm loops. EGW solution, cooled by a low-temperature chiller, acts as a heating medium in tube-in-tube and brazed plate preheaters whereas in small and large condensers it acts as a cooling medium. Liquid enters the test section with three full cone nozzles installed above the tube bundles. Refrigerant gets heated and partially evaporated inside the test section and the vapor goes into the condensers. Liquid refrigerant from condensers and at the bottom of the test section is collected in the receiver. From the receiver, the liquid refrigerant is pumped back into the test section using a variable speed gear pump. Before entering the test box liquid refrigerant passes through a Coriolis mass flow meter and a series of preheaters to achieve the target temperature. The oil is pumped into the preheater inlet using a syringe pump. The separation of oil from the system is achieved by a two-stage oil separation process. A portion of the refrigerant/oil mixture is collected in the primary and secondary separator where it is heated to remove the refrigerant. Oil concentration is measured using the weight sampling method (Peuker and Hrnjak, 2010).



1. Test section (square shell with evaporator tubes inside), 2. Liquid line booster pump, 3. Primary oil separator, 4. Secondary oil separator, 5. Subcooler, 6. Variable speed gear pump, 7. Coriolis mass flow meter, 8. Receiver, 9. Brazed plate preheater, 10. Large condenser, 11. Small condenser, 12. Tube in tube preheater, 13. Electric band heater, 14. Oil syringe pump.

Figure 1: Schematic diagram of the experimental setup.

2.2 Test Procedure

The tests were carried out by using the following main steps:

- 1) Before the start of every series, an overnight leak-tight test is conducted.
- 2) Vacuum the system for about 7 – 8 hours.
- 3) Refrigerant is charged into the system.
- 4) Gear pump is turned on and runs the system bypassing the test section. The flow speed of the pump is adjusted to achieve a steady flow rate. If the flow rate is not steady, repeat step 3 until a steady flow rate is achieved.
- 5) Open the test section and allowed the refrigerant to flow through it.
- 6) Turned on the tube heater and set the required heat flux.
- 7) Data is recorded after the system reaches a steady state.
- 8) Before oil injection, the test is recorded for at least 30 min.
- 9) Calculate the baseline heat transfer coefficient from pre-injection data.

2.3 Oil injection and recovery procedures

The following steps were carried out for the oil injection and recovery processes:

- 1) Estimate the required amount of oil and the oil volume flow rate from the desired OCR value.
- 2) Start the oil injection by setting the oil volume flow rate in the syringe pump.
- 3) Once the system reaches a steady state after oil injection record the data for 30 min.
- 4) After each oil injection test, collect the refrigerant/oil mixture in the primary oil separator.

- 5) Heat the separator for approximately 20 min to remove refrigerant from it.
- 6) Collect the remaining refrigerant/oil mixture in the secondary separator by opening the drain valve on the primary separator.
- 7) Heat the secondary separator to remove the remaining refrigerant from the mixture.
- 8) Record the data for 15 min.
- 9) Calculate the heat transfer coefficient from the data taken at step 8.
- 10) Compare it with the baseline heat transfer coefficient.
- 11) If the value is not in the limits repeat the process from steps 4 to 10.

2.4 Data Reduction and Uncertainty

The average heat transfer coefficient is calculated from the tube wall heat flux, q'' , the average wall temperature, T_w , and the reference temperature T_{ref} as given in Equation (1). T_w is the average wall temperature measured by taking an average of all the thermocouple reading on the tube surface and is given in Equation (2). n is the number of thermocouple readings. T_{ref} was calculated based on the procedures described in Equations (3) and (4). $T_{ref,ees}$ is the reference temperature calculated using the thermodynamic properties in the Engineering Equation Solver (EES) program. Heat transfer factor (HTF) is the ratio of the heat transfer coefficient calculated at oil injection test to the heat transfer coefficient calculated at the baseline test and it is given in Equation(5). The oil circulation ratio (OCR) is the ratio of oil flow rate to the total flow rate and is given in Equation (6). To verify the nominal OCR, weight sampling method is used, and the measured OCR is given in Equation (7). Table 3 gives the uncertainty associated with each measuring device. Uncertainty analysis of HTF is given by Equations (8)-(13). The uncertainty associated with the weight sampling method and nominal OCR measurement is given by Equations (14)-(16) and Equation (17) respectively.

$$h = \frac{q''}{T_w - T_{ref}} \quad (1)$$

$$T_w = \sum_{i=1}^{i=n} \frac{T_i}{n} \quad (2)$$

$$T_{ref} = \begin{cases} \min(T_{in}, T_{sat}) & \text{if } (P_{box} \geq P_{in}) \\ T_{ref,ees} & \text{if } (P_{box} < P_{in}) \text{ and } (T_{in} < T_{sat}) \end{cases} \quad (3)$$

$$T_{ref,ees} = \begin{cases} T_{ref,ees} = T_{out} \\ T_{out} = T @ (h_{out}, P_{box}) \\ h_{out} = h_{in} \\ h_{in} = h @ (T_{in}, P_{in}) \end{cases} \quad (4)$$

$$HTF = \frac{h_{oil}}{h_{baseline}} \quad (5)$$

$$OCR_{nominal} = \frac{\dot{m}_{oil}}{\dot{m}_{oil} + \dot{m}_{refrigerant}} \quad (6)$$

$$OCR_{measured} = \frac{W_{oil}}{W_{sample}} = \frac{W_{oil+beaker} - W_{beaker}}{W_{sample+cylinder} - W_{cylinder}} \quad (7)$$

Table 3: Uncertainty associated with measuring devices.

Device	Accuracy
Box pressure transducer, ΔP_{box}	± 0.0625 psig or 0.13% of FS (50 psig)
Nozzle inlet pressure transducer, ΔP_{in}	± 0.55 psig or 0.11% of FS (500 psig)
Thermocouple, ΔT	$\pm 0.2^\circ\text{F}$
Wattmeter, ΔQ	± 0.02 kW or 0.5% of FS (4kW)
High-capacity refrigerant scale, ΔW_{high}	$\pm 0.5\%$ of reading
Low-capacity scale, ΔW_{low}	± 0.02 g
Coriolis mass flow meter, $\Delta M_{\text{refrigerant}}$	$\pm 0.1\%$ of reading
Oil syringe pump, ΔM_{oil}	$\pm 0.5\%$ of setpoint

$$\delta h = \sqrt{\left(\frac{\delta h}{\delta q''} \Delta q\right)^2 + \left(\frac{\delta h}{\delta T_w} \Delta T_w\right)^2 + \left(\frac{\delta h}{\delta T_{\text{ref}}} \Delta T_{\text{ref}}\right)^2} \quad (8)$$

$$\delta q'' = \frac{\Delta Q}{A} \quad (9)$$

$$\delta T_w = \frac{\Delta T}{\sqrt{n}} \quad (10)$$

$$\delta HTF = \sqrt{\left(\frac{\delta HTF}{\delta h_{\text{oil}}} \Delta h_{\text{oil}}\right)^2 + \left(\frac{\delta HTF}{\delta h_{\text{baseline}}} \Delta h_{\text{baseline}}\right)^2} \quad (11)$$

$$\delta T_{\text{ref}} = \begin{cases} \delta T_{\text{in}} : \text{if } (T_{\text{ref}} = T_{\text{in}}) \\ \delta T_{\text{sat}} : \text{if } (T_{\text{ref}} = T_{\text{sat}}) \\ \delta T_{\text{ref,ees}} : \text{if } (T_{\text{ref}} = T_{\text{ref,ees}}) \end{cases} \quad (12)$$

$$\delta T_{\text{in}} = \Delta T$$

$$\delta T_{\text{sat}} = \text{uncertainty}(P_{\text{in}}) \quad (13)$$

$$\delta T_{\text{ref,ees}} = \text{uncertainty}(P_{\text{in}}, T_{\text{in}}, P_{\text{box}})$$

$$\delta OCR_{\text{measured}} = \sqrt{\left(\frac{\delta OCR}{\delta W_{\text{oil}}} \Delta W_{\text{oil}}\right)^2 + \left(\frac{\delta OCR}{\delta W_{\text{sample}}} \Delta W_{\text{sample}}\right)^2} \quad (14)$$

$$\delta W_{\text{oil}} = \sqrt{\left(\frac{\delta W_{\text{oil}}}{\delta W_{\text{oil+beaker}}} \Delta W_{\text{oil+beaker}}\right)^2 + \left(\frac{\delta W_{\text{oil}}}{\delta W_{\text{beaker}}} \Delta W_{\text{beaker}}\right)^2} \quad (15)$$

$$\delta W_{\text{sample}} = \sqrt{\left(\frac{\delta W_{\text{sample}}}{\delta W_{\text{sample+cylinder}}} \Delta W_{\text{sample+cylinder}}\right)^2 + \left(\frac{\delta W_{\text{sample}}}{\delta W_{\text{cylinder}}} \Delta W_{\text{cylinder}}\right)^2} \quad (16)$$

$$\delta OCR_{nominal} = \sqrt{\left(\frac{\delta OCR}{\delta \dot{m}_{refrigerant}} \Delta \dot{m}_{refrigerant}\right)^2 + \left(\frac{\delta OCR}{\delta \dot{m}_{oil}} \Delta \dot{m}_{oil}\right)^2} \quad (17)$$

The resulting uncertainty from the propagation of error analysis is $\pm 10\%$ in the heat transfer coefficient and in HTF for heat flux of 10 kW/m^2 . The uncertainty decreased to $\pm 6\%$ percent for heat flux of 17 kW/m^2 .

3. RESULTS AND DISCUSSION

A weight sampling method was used as a redundant independent way to measure the lubricant in circulation with the refrigerant during the experiments. The weight sampling method provided a second measurement of the OCR and allowed to verify the OCRs set during the experiments. Representative measurements of the OCRs and associated experimental uncertainties are given in Table 4. The uncertainty associated with the nominal injected OCR are quite low because of the high accuracy of the Coriolis flowmeter used for the refrigerant flow rate and of syringe pump meter used for the lubricant. The weighted sample-based OCR had larger experimental uncertainty due to the precision of the scale used for weighing the tare sampling cylinder. However, the two OCR measurements agreed with each other, confirming that the lubricant pumped into the refrigerant loop remained in circulation during the entire period of the test. Additional tests are planned in future work to confirm the repeatability of the experimental data in Table 4.

Table 4: Results of weight sampling method.

Nominal Injected OCR (%) and measured using Eq. (6)	Measured OCR (%) with weight sample method
0.8 \pm 0.004	1.6 \pm 1.4
1.8 \pm 0.01	2.1 \pm 1.3
1.8 \pm 0.01	2.3 \pm 1.4

The heat transfer coefficient is a function of saturation temperature, inlet subcooling, mass flow rate, and average wall temperature. And it is important to track the change in the above parameters during an oil injection test. Figure 2 shows a variation of system parameters before and after the oil injection. Oil injection time, $\Delta t_{oil \text{ injection}}$, typically lasts about 2 min. The instantaneous readings of the calculated heat transfer coefficient and measured wall temperature, immediately after oil injection are indicated in Figure 2. Except for average wall temperature, the variations in the other system quantities were small during an oil injection test.

HTF of POE68/R134a mixture at OCR of 2% at saturation temperatures of -6°C (20°F), 2°C (36°F), and 10°C (50°F), is shown in Figure 3. HTF decreases with an increase in heat flux. This is because of partial dry out of tubes and an increase of the oil-rich film around the tube wall, resulting in higher thermal resistance, when the heat flux increased. A significant decrease in HTF is observed with the addition of oil at -6°C (20°F). Figure 4 shows the variation of HTF of POE68/R1234ze(E) mixture at OCR of 1- 2% at saturation temperatures of -6°C (20°F), 2°C (36°F), and 10°C (50°F). Compared to figure 3, a similar trend is observed. However, at a lower OCR of 1%, at higher heat flux and increase in HTF is observed.

HTF of POE220/R1234ze(E) and PE100/R1234ze(E) mixtures at OCR of 1-2% at a saturation temperature of 2°C (36°F) is shown in Figure 5. As mentioned before, HTF decreases with an increase in heat flux at a higher OCR of 1.5 or 2%. However, at a lower OCR of 1%, for PE100, there is a slight increase in the HTF is observed at the highest heat flux. Compared to polyester (POE) type oil, HTF of polyether (PE) is much lower at the same heat flux and OCR. The viscosity and solubility characteristics of oil has a major role in HTF. Figure 6 shows the variation of HTF with R1234ze(E)/oil mixtures having different viscosities. It is clear from the figure that PE-type oil has more damaging effects on HTF compared to POE-type oil. Decrease in HTF for high viscosity PE-type oil may be due to its poor solubility and a further investigation is required. An increase in HTF is observed with an increase in oil viscosity by comparing the POE type oil. Higher viscosity of oil increases the surface tension of the refrigerant. Greater surface tension would cause foaming which makes easier to wet the tube and the same is reported in Minxia *et al.* (2021).

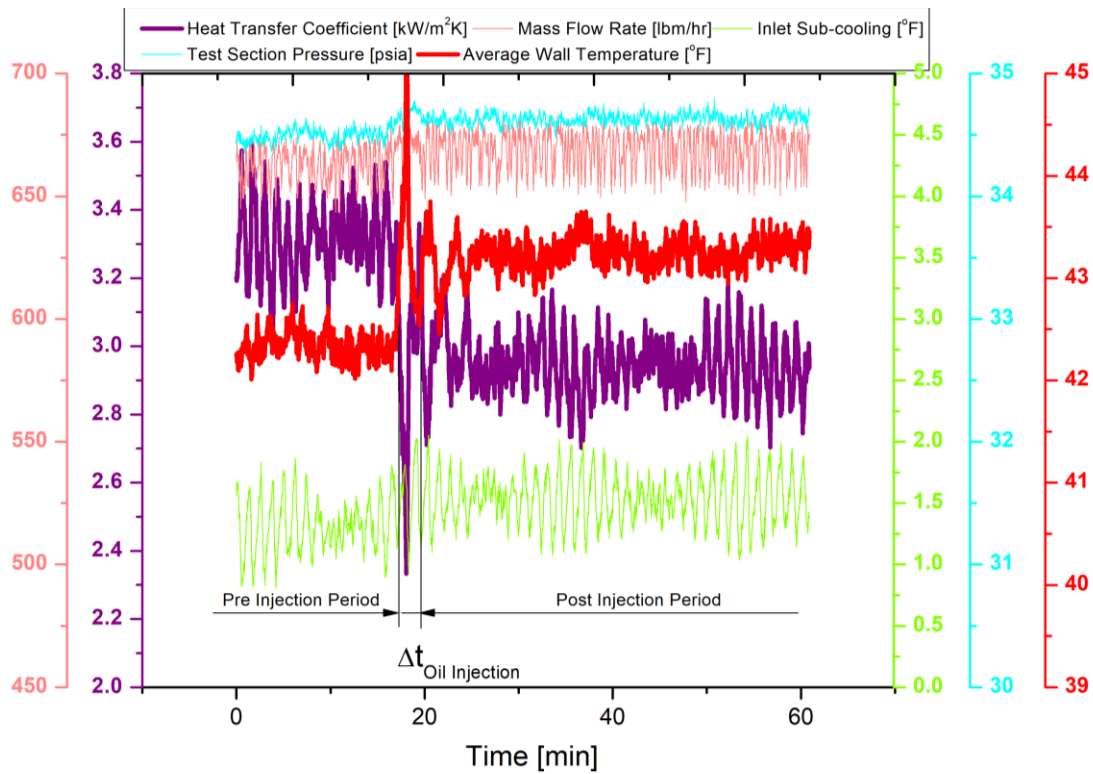


Figure 2: Variation of HTC, mass flow rate, inlet subcooling, box pressure and average wall temperature during an oil injection test.

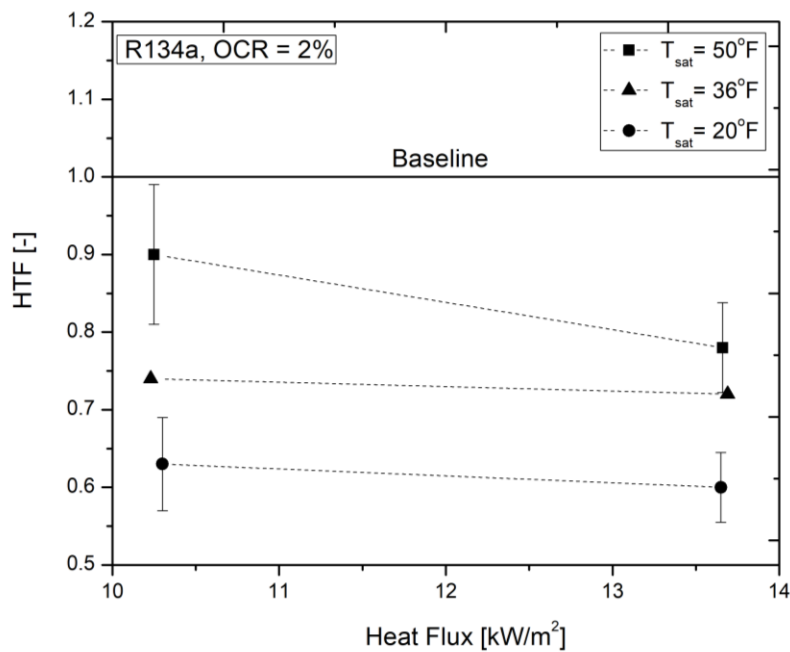


Figure 3: Variation of HTF with heat flux of R134a/POE68 mixture.

Most of the new data measured in the present work were aligned with similar observations from the published literature in that spray evaporation of R245fa/oil mixture by Chien *et al.* (2019), who reported a decrease in HTC with heat flux

at OCR higher OCR of 4.8%. Similarly, in pool boiling experiments of R1234ze(E)/POE68 (Kumar and Wang, 2022) a degradation in HTC was observed at 5% OCR while an enhancement in HTC was reported at 2% OCR. Some discrepancies were observed between the present study and the study by Minxia *et al.* (2021) were they reported a higher HTC at higher OCR of 5.1%. This may be due to the bundle effect in the present study and further investigation is required in future work.

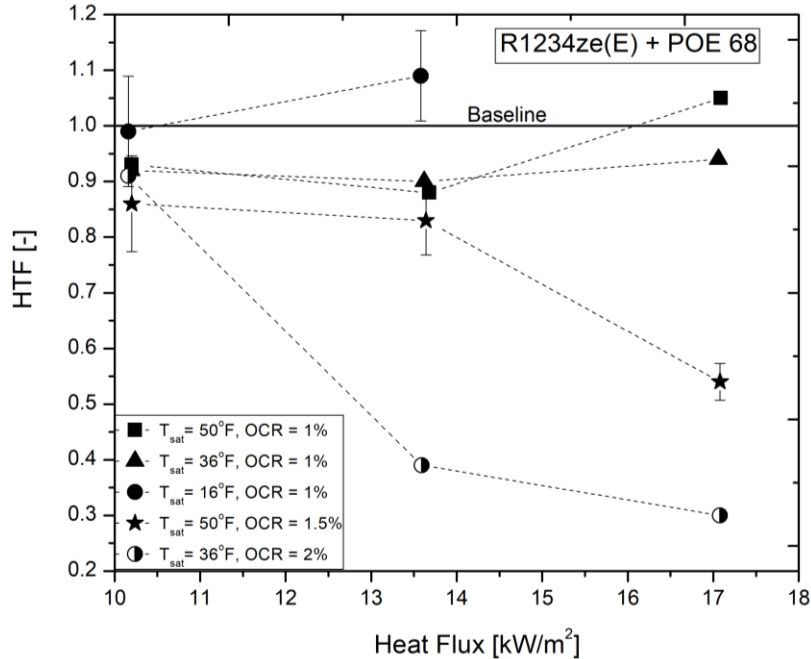


Figure 4: Variation of HTF with heat flux of R1234ze(E)/POE68 mixture.

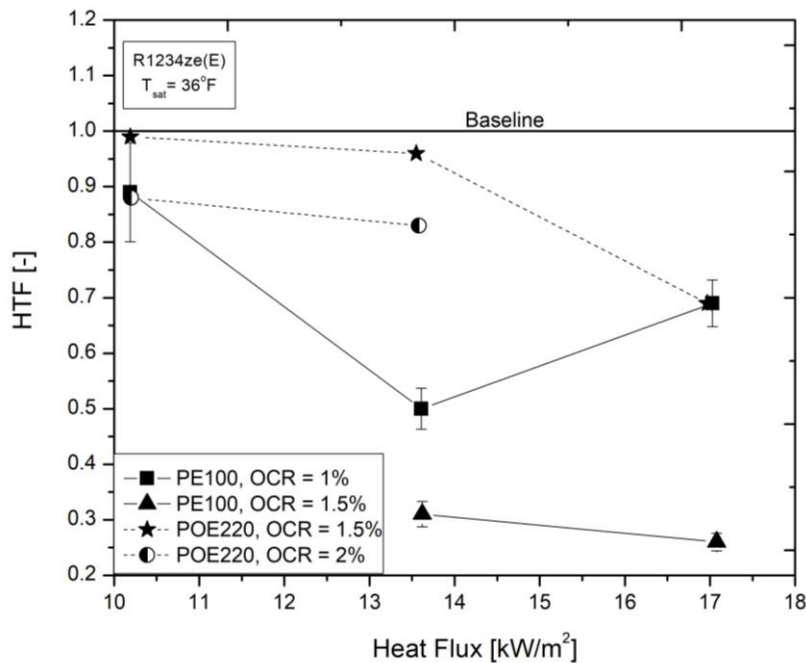


Figure 5: Variation of HTF with heat flux of R1234ze(E)/POE220 and R1234ze(E)/PE100 mixtures.

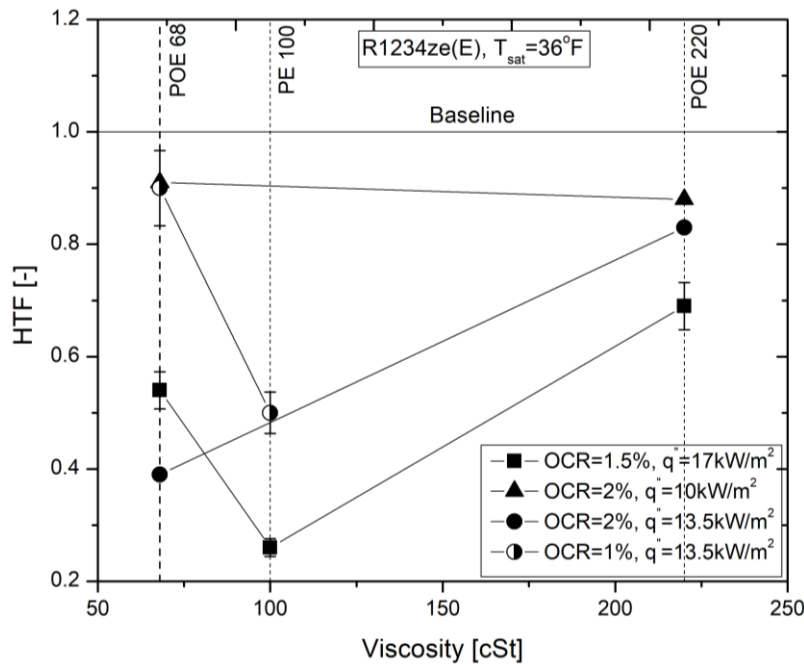


Figure 6: Variation of HTF with oil viscosity.

4. CONCLUSIONS

This paper describes an experimental investigation of the effect of lubricating oil on the heat transfer performance of spray evaporators for air conditioning and refrigeration systems. The experiments were carried out for refrigerant and lubricant mixtures of R134a and R1234ze(E) with synthetic polyester (POE) and polyether (PE) lubricants. The saturation temperature ranged from -9°C to 10°C (16°F to 50°F), and the heat flux varied between 3 kW/m^2 and 20 kW/m^2 . Most of the new data measured in the present work were aligned with similar observations from the published literature. Some discrepancies were observed between the present study and one study published in the literature and it may be due to the bundle effects occurring with the tube bundle setup of the present study. The specific conclusions from the present study are as follows:

- The effect of oil circulating with the refrigerant has a significant effect on the wall temperature of the evaporator tubes.
- At high OCRs of 1.5-2% the HTF decreases with an increase in heat flux for both R134a/POE68 and R1234ze(E)/POE68 mixtures. However, at a lower OCR of 1%, an increase in HTF was observed at the highest heat flux for the R123ze(E)/POE68 mixture.
- HTF of R1234ze(E)/POE68 mixture, at the same heat flux and OCR, decreases if the saturation temperature is lowered.
- Compared to POE/refrigerant mixture, at the same heat flux and OCR, the HTF is much lower in the PE/refrigerant mixture. For the POE/refrigerant mixtures, the HTF increases with an increase in the viscosity of the base lubricating oil.

NOMENCLATURE

GWP	global warming potential	(-)
HFO	hydrofluoro-olefins	(-)
OCR	oil circulation ratio	(-)
PE	polyether	(-)
POE	polyester	(-)
EGW	ethylene glycol water	(-)
HTC	heat transfer coefficient	($\text{W/m}^2\text{K}$)

HTF heat transfer factor (–)

REFERENCES

- Ribatski, G., & Jacobi, A. M. (2005). Falling-film evaporation on horizontal tubes—a critical review. *International journal of refrigeration*, 28(5), 635-653.
- Jin, P. H., Zhao, C. Y., Ji, W. T., & Tao, W. Q. (2018). Experimental investigation of R410A and R32 falling film evaporation on horizontal enhanced tubes. *Applied Thermal Engineering*, 137, 739-748.
- Pecherkin, N., Pavlenko, A., Volodin, O., Kataev, A., & Mironova, I. (2021). Experimental study of heat transfer enhancement in a falling film of R21 on an array of horizontal tubes with MAO coating. *International Communications in Heat and Mass Transfer*, 129, 105743.
- Ji, W. T., Zhao, E. T., Zhao, C. Y., Zhang, H., & Tao, W. Q. (2019). Falling film evaporation and nucleate pool boiling heat transfer of R134a on the same enhanced tube. *Applied Thermal Engineering*, 147, 113-121.
- Van Rooyen, E., & Thome, J. R. (2013). Pool boiling data and prediction method for enhanced boiling tubes with R-134a, R-236fa and R-1234ze (E). *International journal of refrigeration*, 36(2), 447-455.
- Nagata, R., Kondou, C., & Koyama, S. (2016). Comparative assessment of condensation and pool boiling heat transfer on horizontal plain single tubes for R1234ze (E), R1234ze (Z), and R1233zd (E). *International Journal of Refrigeration*, 63, 157-170.
- Byun, H. W., Kim, D. H., Yoon, S. H., Song, C. H., Lee, K. H., & Kim, O. J. (2017). Pool boiling performance of enhanced tubes on low GWP refrigerants. *Applied Thermal Engineering*, 123, 791-798.
- Ji, W. T., Xiong, S. M., Chen, L., Zhao, C. Y., & Tao, W. Q. (2021). Effect of subsurface tunnel on the nucleate pool boiling heat transfer of R1234ze (E), R1233zd (E) and R134a. *International Journal of Refrigeration*, 122, 122-133.
- Jige, D., Miyata, H., & Inoue, N. (2019). Falling film evaporation of R1234ze (E) and R245fa on a horizontal smooth tube. *Experimental Thermal and Fluid Science*, 105, 58-66.
- Ouyang, X. P., & Sun, K. (2022). Falling film evaporation experiment and data processing method of R1234ze (E) on horizontal enhanced tubes. *International Journal of Refrigeration*, 134, 45-54.
- Ubara, T., Asano, H., & Sugimoto, K. (2021). Falling film evaporation and pool boiling heat transfer of R1233zd (E) on thermal spray coated tube. *Applied Thermal Engineering*, 196, 117329.
- Hassani, M., & Kouhikamali, R. (2020). Heat and mass transfer modeling of R-245fa and R1233zd (E) with concurrent boiling and convective evaporation in falling film applications. *International Journal of Refrigeration*, 117, 181-189.
- Bandarra Filho, E. P., Cheng, L., & Thome, J. R. (2009). Flow boiling characteristics and flow pattern visualization of refrigerant/lubricant oil mixtures. *International journal of refrigeration*, 32(2), 185-202.
- Bolaji, B. O., & Huan, Z. (2013). Ozone depletion and global warming: Case for the use of natural refrigerant—a review. *Renewable and Sustainable Energy Reviews*, 18, 49-54.
- Gibb, P., Randles, S., Millington, M., & Whittaker, A. (2003). Lubricants for sustainable cooling. In: *Proceedings of the 2003 CIBSE/ASHRAE conference*, Edinburgh, United Kingdom.
- Chien, L. H., Tsai, Y. L., & Chang, C. H. (2019). A study of pool boiling and falling-film vaporization with R-245fa/oil mixtures on horizontal tubes. *International Journal of Heat and Mass Transfer*, 133, 940-950.
- Li, Y., Li, M., Li, Y., Cai, W., & Yao, L. (2021). Experimental investigation on the heat transfer performance of falling film evaporation with lubrication oil on horizontal tubes having different structures. *International Journal of Thermal Sciences*, 160, 106669.
- Peuker, S., & Hrnjak, P. S. (2010). Experimental techniques to determine oil distribution in automotive A/C systems. *13th International Refrigeration and Air Conditioning Conference*, Purdue University, West Lafayette, Indiana, USA.
- Kumar, A., & Wang, C. C. (2022). Nucleate pool boiling heat transfer of R-1234ze (E) and R-134a on GEWA-B5H and smooth tube with the influence of POE oil. *Applied Thermal Engineering*, 201, 117779.

ACKNOWLEDGEMENT

We are thankful to ASHRAE for supporting the research project RP-1800. Thanks to ASHRAE Technical Committees TC 1.3 and 8.5 and the Project Monitor Subcommittee of ASHRAE RP-1800 for their technical help and consultation with the project RP-1800. Thanks to Josh Rothe (Ph.D. student at Auburn University) for his help with the experimental setup and calibration.